Journal of Solid State Chemistry 184 (2011) 2209–2214

Contents lists available at ScienceDirect

Journal of Solid State Chemistry

journal homepage: www.elsevier.com/locate/jssc

Low cost, surfactant-less, one pot synthesis of Cu_2O nano-octahedra at room temperature

Asar Ahmed [a], Namdeo S. Gajbhiye [a,*], Amish G. Joshi [b]

[a] Department of Chemistry, Indian Institute of Technology Kanpur, Kanpur 208016, Uttar Pradesh, India
[b] Physics of Energy Harvesting Division, National Physical Laboratory, Dr. K.S. Krishnan Road, New Delhi 110012, India

ARTICLE INFO

Article history:
Received 14 February 2011
Received in revised form
26 May 2011
Accepted 29 May 2011
Available online 25 June 2011

Keywords:
Cu_2O
D-Glucose
Octahedra
Hydrazine
XPS

ABSTRACT

Cu_2O octahedra were successfully synthesized via a novel wet-chemical method using D-glucose and hydrazine as reducing agent at room temperature without the presence of any other surfactant. Presence of D-glucose was important for the stabilization of the evolved copper octahedra and also for facilitating the reduction of the Cu(II) ions. The existence of glucose moieties on the surface as capping agent was confirmed by the FT-IR spectra while there was presence of excess oxygen atoms on the surface leading to the formation of a thin CuO layer at the octahedra surface, as confirmed by the XPS study, probably promoted by the capping glucose. Effect of NaOH concentration on the reaction and the formation of octahedra was also studied. The formation mechanism of obtained Cu_2O octahedra has been discussed. These octahedra were then studied for their photocatalytic properties in degradation of organic dyes, rhodamine B and methyl orange.

1. Introduction

In recent times, there has been extensive interest among the material scientists in tailoring the structure of nanomaterials for developing specific morphologies [1–6]. These materials with different morphologies often exhibit new physical and chemical properties which differ from their spherical counterpart as the shape and size of the nanomaterials are well known to have great influence on their widely varying properties [7,8]. Their unique structures and properties may lead to a wide variety of applications. Semiconductor nanomaterials with different morphologies such as nanowires, nanorods [9,10], nanocubes [11], hollow spheres [12], tetrapods [13,14] have been synthesized in the recent times for their interesting properties and their potential applications. However, the preparation of nanomaterials of highly symmetric platonic shapes including tetrahedron, octahedron, hexahedron (cube), icosahedron and dodecahedron is still a great challenge.

Cuprous oxide, a p-type semiconductor with a direct band gap of 2.17 eV [15], has attracted much current research interest because of its numerous advantages such as non-toxicity, low cost, easy availability, high optical absorptions coefficients in the range of $2\times10^5-3.7\times10^6$ cm^{-1} were found for photon energies higher than 2.7 eV and theoretical energy conversion efficiency greater than 20%, in both bulk and in the nanomaterial form which makes it a promising material for various types of applications [16–19]. It has potential to form high efficiency solar cells with high open-circuit voltage by combination with a suitable n-type semiconductor to able to convert solar energy into electrical or chemical energy [20]. It was reported to act as a good catalyst for water splitting when irradiated with visible light [21]. It has been used in gas sensor technology for detecting various kinds of molecules [22]. It is a material which can be used for photodegradation of dye molecules [23] and in the environmental applications also, such as for CO oxidation [24]. Several reports in the recent times have proved that Cu_2O nanomaterials can be used as the negative electrode material in the lithium ion batteries [25]. There exists a wide variety of different shapes and sizes of Cu_2O nanostructures e.g. hollow spheres [26], nanocages [27], nanocubes [28] and other special type structures [26,29,30] prepared by a number of different synthetic methodology, such as vacuum evaporation [31], sonochemical method [32], thermal relaxation [33], liquid phase reduction [34] and electrodeposition [35].

Although several synthetic strategies have been demonstrated for the preparation of Cu_2O octahedra with different sizes and shapes, most of them involve preparation at high temperature, multi-step sample preparation processes, and/or with the use of organic solvents [36,37]. Moreover in these methods, surfactants such as Polyethyelene Glycol (PEG), Cetyltrimethyl Ammonium Bromide (CTAB) or Sodium Dodecyl Sulfate (SDS) were generally required to control the morphologies and structures of the

* Correspondence to: SL-214, Southern Laboratories, Department of Chemistry, Indian Institute of Technology Kanpur, Kanpur 208016, Uttar Pradesh, India.
E-mail address: nsg@iitk.ac.in (N.S. Gajbhiye).

0022-4596/$ - see front matter © 2011 Elsevier Inc. All rights reserved.
doi:10.1016/j.jssc.2011.05.058

material. So, it is necessary to develop an effective and facile method for the controlled synthesis of a perfect Cu_2O nanocrystal with high yield without any surfactant. Developing effective and facile methods for the controlled synthesis of octahedral Cu_2O as well as investigating the corresponding growth mechanism are still needed. Herein we report, a simple one-pot solution phase synthesis of Cu_2O octahedra of dimension of about 100–150 nm from cupric sulfate precursor in the presence of D-glucose and hydrazine hydrate under alkaline conditions at room temperature. Here, D-glucose is utilized to perform multiple tasks; to stabilize the surface of the evolved particles by acting as capping agent and to facilitate the reduction of Cu(II) ions. The synthesis does not require the assistance of any organic compounds or surfactants. It was also found out that at a particular concentration of the D-glucose, well-defined octahedra are obtained. Also, the formation of Cu_2O octahedra is highly dependent on the various reaction conditions. The morphology and size of Cu_2O can be easily controlled by adjusting the concentration of D-glucose solution and NaOH solution. The mechanism for the formation of octahedral Cu_2O nanoparticles has been discussed. These octahedra nanoparticles were then studied for their photocatalytic properties in the degradation of organic dyes. Photodegradation of rhodamine B and methyl orange were carried out to prove the potential catalysis of the synthesized nanomaterials.

2. Experimental

2.1. Chemicals used

Cupric sulphate pentahydrate ($CuSO_4 \cdot 5H_2O$), D-glucose, NaOH, hydrazine hydrate ($N_2H_4 \cdot H_2O$), rhodamine B, methyl orange and ethanol were purchased from S.D. Fine Ltd. (India) and used as-received without further purification. All of the chemical reagents used in this experiment were of analytical grade.

2.2. Procedure

Cu_2O octahedra were synthesized as follows: 0.5 g of $CuSO_4 \cdot 5H_2O$ (2 mmol) and 0.361 g of D-glucose (2 mmol) were completely dissolved in 100 mL of double distilled water in a 250 mL round bottom flask fitted with Ar gas flow and started magnetic stirring. After 15–20 min of stirring, 2 mL of 10 M NaOH was added in a drop wise manner with the help of dropping funnel into the solution and a blue colored solution of $Cu(OH)_2$ was soon produced. After stirring for 30 min, 3 mL of 2 M $N_2H_4 \cdot H_2O$ solution was dropped into this solution, color of the solution gradually changed from blue to brick red. The solution was stirred until the $Cu(OH)_2$ precipitates were completely reduced by the hydrazine hydrate. The brick red precipitates were collected by centrifugation at 8000 rpm for 30 min, washed with methanol (HPLC grade) several times and centrifuged afterwards. Then it was dried in vacuum oven at 60 °C for 3 h.

The photodegradation of rhodamine B and methyl orange dyes by the as-synthesized Cu_2O octahedra was studied. In the case of rhodamine N dye, 0.1 g sample of Cu_2O octahedra was dispersed in a 50 mL of aqueous rhodamine B solution (10 ppm) and was stirred magnetically in the dark for 45 min to reach adsorption equilibrium. Then the solution was irradiated with UV/vis light from the mercury lamp. The concentrations of rhodamine B were measured after every 1 h by the UV–vis spectroscopy. In the case of methyl orange, 0.05 g sample of Cu_2O octahedra was dispersed in a 50 mL of aqueous methyl orange solution (10 ppm) and was stirred magnetically in the dark for 45 min to reach adsorption equilibrium. Then the solution was exposed to sunlight. The concentrations of methyl orange were measured after every 1 h by the UV–vis spectroscopy. Blank tests i.e. rhodamine B and methyl orange without any catalyst under the same other conditions were also conducted. Experiments done in dark under other same conditions were also carried for both rhodamine B and methyl orange.

2.3. Instrumentation

The powder X-ray diffraction measurements were carried out on a Rich Seifert Isodebyflex X-ray unit model 2002 with Cu $K\alpha$ radiation and Ni-filter in the 2θ range of 35–120°. Scanning Electron Microscopy (SEM) was done by using JEOL JSM-840 A machine and Field Emission Scanning Electron Microscopy (FESEM) images were taken by Ziess, Supra-40VP instrument. Fourier Transform Infra-red (FTIR) spectra were recorded by Brooker Vertex-70 spectrophotometer and Fluorolog (R)-3 Spectrofluorometer was used to collect the photoluminescence spectra. X-ray Photoelectron Spectroscopic (XPS) measurements were performed in an ultra-high vacuum chamber (PHI 1257) with a base pressure of $\sim 4 \times 10^{-10}$ Torr. The XPS spectrometer was equipped with a high resolution hemispherical electron analyzer (279.4 mm diameter with 25 meV resolution) and a Mg ($K\alpha$) ($h\nu = 1253.6$ eV) X-ray excitation source. All the spectra were referenced to adventitious C (1*s*) at 284.5 eV binding energy (BE). The UV–visible spectroscopy was performed on Systronics Double Beam Spectrophotometer instrument. The photocatalytic activity was evaluated under UV–vis irradiation from a 500 W mercury lamp.

3. Results and discussion

The powder XRD pattern of the Cu_2O octahedra is given in Fig. 1. There are four clear peaks in the figure. All of them can be perfectly indexed to a single phase of crystalline Cu_2O (JCPDS No. 78-2076), not only in peak position, but also to their relative intensity, and the results presented here coincided with the literature values. The peaks with 2θ values are 37.7402°, 43.6758°, 62.8232° and 75.0440° which corresponds to the crystal planes of (1 1 1), (2 0 0), (2 2 0) and (3 1 1) of crystalline Cu_2O, respectively. From the XRD data, the average crystallite size was calculated between 21 and 30 nm for different samples using Scherrer's equation. The morphology and size of the product was studied by electron microscopy techniques. The FESEM images in Fig. 2a–e clearly show the general morphology of the synthesized Cu_2O nanomaterial in this work. After examination of the images, we find that majority of the Cu_2O nanocrystals have the octahedral structure and the size of these octahedra are in the range of 100–150 nm. The geometrical symmetry of the as-synthesized octahedra was further elucidated by TEM (Fig. 2f). The samples

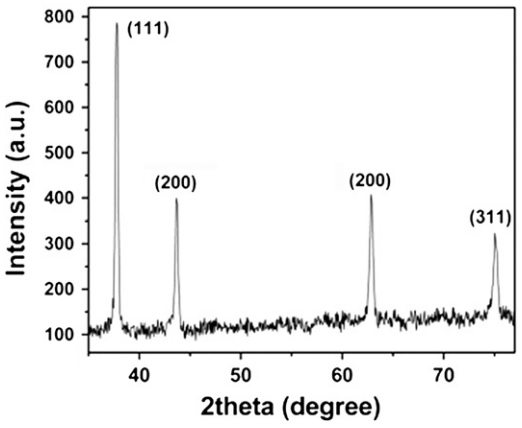

Fig. 1. Powder XRD pattern.

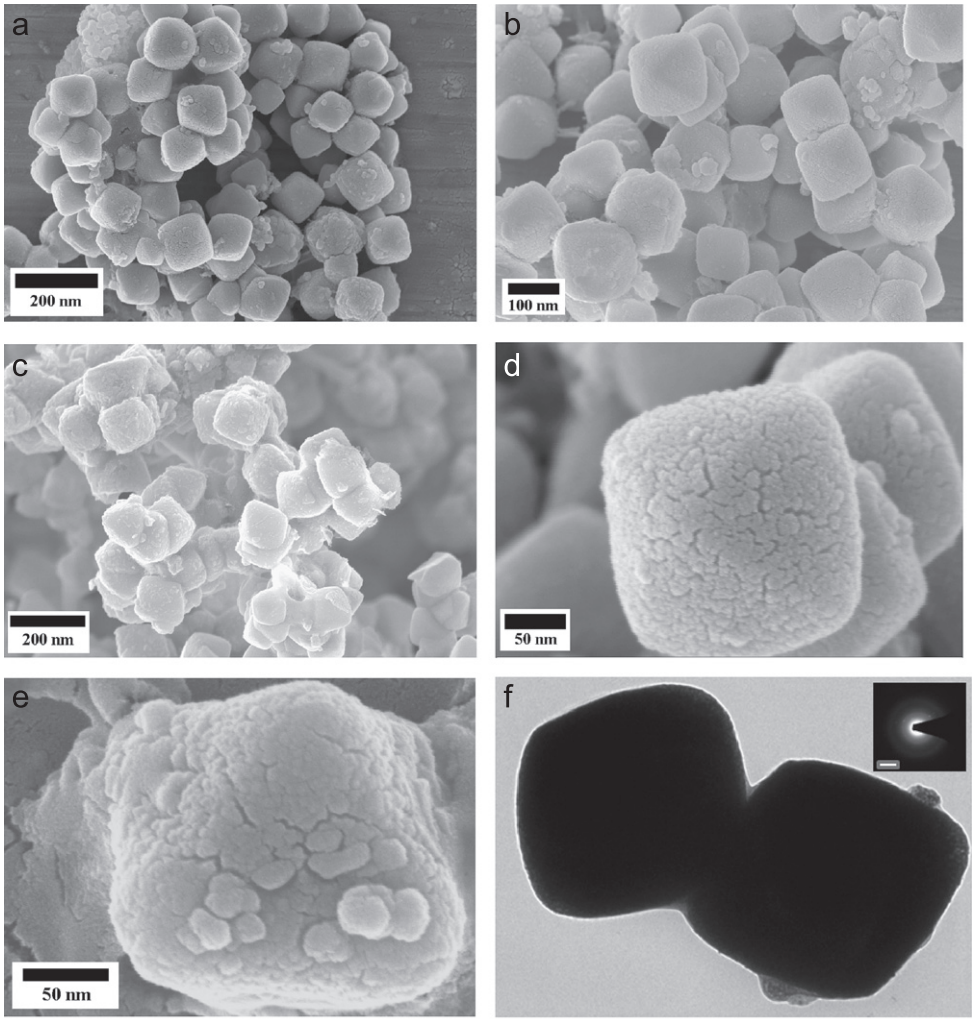

Fig. 2. Electron microscopy images of the samples. (a) FE-SEM image; (b) FE-SEM image; (c) FE-SEM image; (d) high resolution FE-SEM image; (e) FE-SEM image of the broken octahedra; and (f) TEM image (SAED pattern in inset with bar scale 5 1/nm).

were ultra-sonicated for around 2 h and were found to have broken partially as displayed in Fig. 2e giving rise to smaller nanoparticles, therefore proves that the octahedra constituted of primary nanoparticles of lower dimensions.

The FT-IR spectrum of the samples (Fig. 3) exhibits characteristic band at 621 cm^{-1} which corresponds to the optically active lattice vibration of Cu_2O, therefore further confirms the single crystalline pure phase nature of the metal oxide [38]. FT-IR spectrum of the Cu_2O octahedra samples are compared with the spectrum of D-glucose. The changes in the infra-red spectra of the samples are similar to the earlier reported literature [39]. The bands in the regions 3000–3700 and 2800–3000 cm^{-1} due to the OH stretching and CH stretching undergo major modifications. The intensities of different bands in the CH stretching are highly affected and the bands are shifted to higher frequencies by 10–15 cm^{-1}. Similarly the 700–1700 cm^{-1} region was also affected and the intensity of the band at 630 cm^{-1} due to CH_2 vibration is increased considerably due to the contribution of the Cu–O band in this region. The high stability of the colloidal solution of Cu_2O in water indicates the presence of hydrophilic groups on the surface of the octahedra. The synthesized nanomaterials were stable for more than 10 days, which further indicates that the stabilization of the octahedra was due to the capping by D-glucose/gluconic acid molecules on the surface. Therefore the FT-IR results confirm the presence of the D-glucose molecule on the surface of the nanoparticles even after

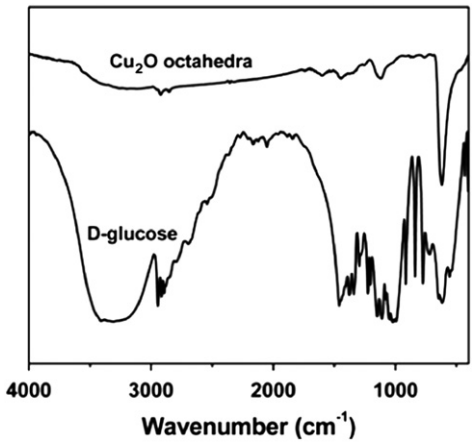

Fig. 3. FT-IR spectrum of Cu_2O octahedra and D-glucose.

washing the samples thoroughly many times with methanol, providing directionality for the growing nanocrystals to produce the special shape and stabilizing the surface of the octahedra through the co-ordinative interactions between the oxygen atoms present in the hydrophilic part of the D-glucose molecule and the surface of the resulting Cu_2O octahedra.

The presence of the excess oxygen atoms in the form of cupric oxide thin layer on the surface of the octahedra was corroborated by the XPS analysis. The core level Cu $2p_{3/2}$ spectra was analyzed after deconvolution as shown in Fig. 6. The main peak is relatively broad, has a binding energy of 932.95 eV, with primarily $2p^3\ d^{10}L$ character, where $2p$ and L represents a hole in the core and ligand shell, respectively. A satellite peak was also seen at about 942.15 eV mainly with $2p^3d^9$ character [40]. This satellite is the signature characteristics of d^9 configuration for materials like copper dihalides, cupric oxide or metallic nickel in the ground state. The Coulomb repulsion between the core hole and the $3d$ hole leads to higher binding energy. While in the Cu_2O, the d shell is full and screening via a charge transfer into the d states cannot occur therefore satellite peak should not be observed in Cu_2O but in our work satellite peak was discovered, thus confirms the existence of a thin surface layer of cupric oxide. As existence of excess oxygen atoms on the surface could be verified from the XPS analysis, therefore we can say that those oxygen atoms from D-glucose had strong coordinative interactions with the exposed Cu atoms present on the Cu_2O surface which subsequently encourage the oxidation of the surface Cu atoms from the +1 oxidation state to the more stable +2 oxidation state, leading to the formation of thin layer of the oxidized Cu(II) species on the surface. However, it must be noted that as a surface analyzing tool, XPS is sensitive to information coming from 1 to 2 nm surface layer as it is the depth from which the photoelectron can escape. The monoclinic CuO could not be detected by the powder XRD spectra which exhibited no peaks corresponding to CuO, therefore indicating the very thin layer of CuO. Also due to the lower symmetry of the monoclinic CuO compared with cubic Cu_2O, XPS over-estimates the ratio of CuO [41], therefore we could say that the percentage of Cu(II) state was much lower than observed from the XPS technique and the intensities corresponding to the Cu^{2+} and Cu^{1+} do not precisely reflect the ratio of them in the sample.

Photoluminescence spectroscopy is an effective tool to study the electronic properties of the samples. To observe the different transitions between the higher sub levels of the conduction band and the Cu d-shell of the valence band, the sample were excited at 340 nm wavelength at room temperature. Photoluminescence spectrum in Fig. 4 clearly shows strong emission bands at 435 and 416 nm, an obviously blue-shift emission as compared to the bulk PL spectrum which shows a maximum peak around 570 nm. It may be argued that the blue-shift was caused due to the quantum confinement of exciton photogenerated inside the nanostructured octahedra and the broadening of the peak as compared to the bulk is in agreement with the smaller crystallite size.

The concentration of NaOH has much influence on the reaction rate. If OH^- concentration is not high enough, the conversion to hydroxide is very slow which in turn effects the formation of octahedra formation. In high OH^- concentration, the reaction can be carried out spontaneously 10 min more or less even after the addition of D-glucose without the addition of hydrazine. In the present system, we propose, NaOH may also act as an activator. Preparation of Cu_2O octahedra is successful only under highly alkaline conditions (pH=12.20) when using cupric sulfate as the precursor in the presence of D-glucose, NaOH and hydrazine hydrate. Under the alkaline medium, cupric sulfate was easily converted into the cupric hydroxide, which was responsible for nucleation and successive growth, and was readily reduced to Cu_2O by the addition of hydrazine hydrate at the room temperature. At the lower pH values, D-glucose is neutral, therefore has lower capability for forming complexes with copper ions. At higher pH values, α-D-glucose transforms into β-D-glucose through the open chain form, which is reactive and this phenomenon is called as mutarotation. The schematic reaction mechanism and the reactions are displayed in Fig. 5. The open chain structure gets converted to gluconic acid in the alkaline medium by oxidation of the free aldehyde group to carboxylate form.

D-glucose performs multiple roles in the preparation of Cu_2O octahedral in this study. Copper ions are stabilized by forming Cu–glucose/Cu–gluconic complexes, which leads to the formation of nanomaterials. D-glucose, like other sugars such as fructose, also facilitates the reduction of Cu(II) ions. As the reducing ability of D-glucose is much weaker than that hydrazine, its reduction effect on the formation of Cu_2O octahedra cannot be negligible only at relatively high D-glucose concentrations. At low D-glucose concentrations, D-glucose only plays a role in stabilizing copper ions. In the reaction solution, the presence of D-glucose was the most important factor in determining the morphology of the final product as substituting it with surfactants like SDS, did not give desired

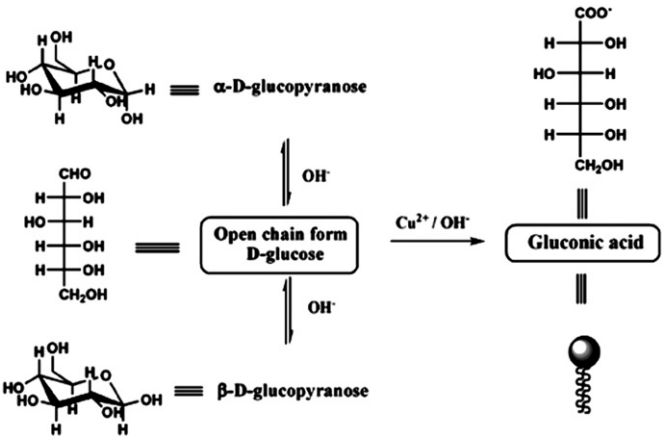

Fig. 5. Mechanism for the formation of Cu_2O octahedra.

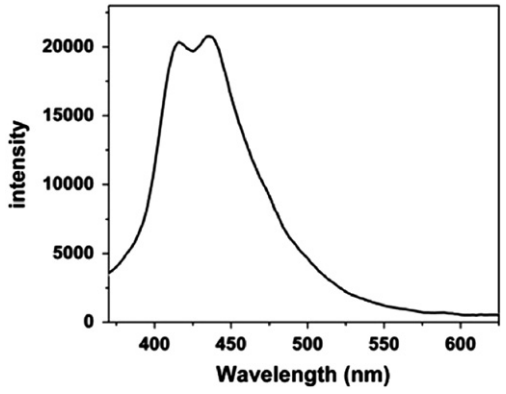

Fig. 4. Photoluminescence spectrum.

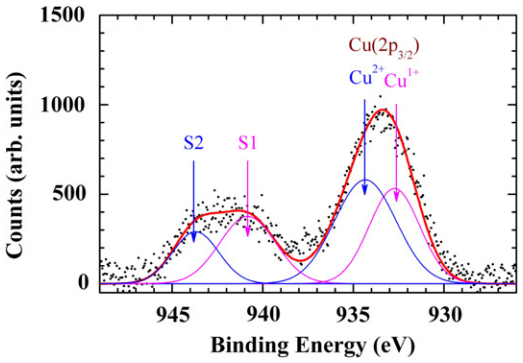

Fig. 6. De-convoluted spectrum of core level Cu $2p$ 3/2.

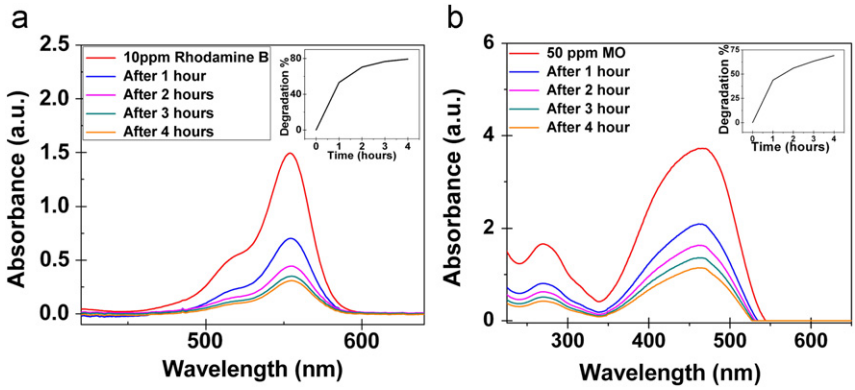

Fig. 7. Photocatalytic activity of Cu_2O. (a) Degradation of rhodamine B dye and (b) degradation of methyl orange.

morphology. With the assistance of D-glucose in the alkaline medium, the finer cuprous oxide nanoparticles were able to grow into octahedral shaped structures, by kinetically controlling the growth rates of various faces of the octahedron. It could be believed that when glucose is introduced, there was a selective interaction between the glucose molecule and the various crystallographic planes of Cu_2O, following by the reduction in the growth rate along the $\langle 1\,1\,1 \rangle$ direction and enhancement of the growth rate along the $\langle 1\,0\,0 \rangle$ direction, therefore, the most stable (1 1 1) faces preferentially appear and the octahedron geometry was obtained.

Photocatalysis of the as-synthesized nanomaterials was also studied for the degradation of organic dyes rhodamine B and methyl orange. The photodegradation of rhodamine B and methyl orange are shown in Fig. 7a and b, respectively. The photocatalytic activity of Cu_2O is displayed in the inset is represented as the degradation percentage which was calculated as the % of organic dye degraded with respect to its initial concentration. After one hour of UV–vis light irradiation, rhodamine B was degraded more than 50% by the Cu_2O octahedra. After 4 h of UV–vis light illumination, the degradation of the dye reached almost 80%. While in the case of dye methyl orange, it was shined with sunlight to observe the photodegradation. After one hour of sunlight exposure, the dye was degraded up to 44% which reached almost 70% degradation after 4 h of continuous sunlight exposure. Blank tests i.e. rhodamine B and methyl orange without any catalyst exhibited negligible degradation which means that photodegradation of these dyes was extremely slow in the absence of catalyst. The degradation of rhodamine B and methyl orange by Cu_2O octahedra in darkness was also similar. Thus it may be concluded that the degradation of the dyes by Cu_2O was due to the photocatalysis involving Cu_2O. The photocatalytic activity of the octahedra was found to be very promising for the degradation of toxic organic dyes.

4. Conclusion

In summary, Cu_2O octahedra have been synthesized by a simple one-pot solution phase method at room temperature in the presence of D-glucose, without the addition of any other surfactant. Presence of D-glucose was important for the stabilization of the growing nanoparticles as a capping agent, to facilitate the reduction of Cu(II) ions and to kinetically control the growth rates of various faces leading to the octahedron geometry. The existence of glucose moieties on the surface as capping agent was confirmed by the FT-IR spectroscopy. XPS study clearly confirms the presence a thin layer of CuO at the octahedra surface, probably promoted by the capping glucose. Effect of NaOH concentration on the reaction and the formation of octahedra was also studied. The mechanism for the formation of octahedral Cu_2O nanoparticles has been discussed. The detailed mechanism for the octahedra formation involving D-glucose needs to be further investigated. Photodegradation of the organic dyes catalyzed by these nanomaterials was found to be very promising.

Acknowledgments

Authors acknowledge financial support from Department of Science and Technology (DST), India. One of the authors (AA) thanks the University Grants Commission (UGC), New Delhi for the award of Senior Research Fellowship.

References

[1] Y. Xie, J.X. Huang, B. Li, Y. Liu, Y.T. Qian, Adv. Mater. 12 (2000) 1523–1526.
[2] J.T. Sampanthar, H.C. Zeng, J. Am. Chem. Soc. 124 (2002) 6668–6675.
[3] P.V. Braun, P. Osenar, S.I. Stupp, Nature 380 (1996) 325–328.
[4] X.W. Lou, H.C. Zeng, J. Am. Chem. Soc. 125 (2003) 2697–2704.
[5] S. Iijima, Nature 354 (1991) 56–58.
[6] P.C. Ohara, J.R. Heath, W.M. Gelbart, Angew. Chem. Int. Ed. Engl. 36 (1997) 1078–1080.
[7] A.P. Alivisatos, Science 271 (1996) 933–937.
[8] M.A. El-Sayed, Acc. Chem. Res. 34 (2001) 257–264.
[9] Y.N. Xia, P.D. Yang, Y.G. Sun, Y.Y. Wu, M.B. Gates, Y.D. Yin, F. Kim, H.Q. Yan, Adv. Mater. 15 (2003) 353–389.
[10] N.S. Gajbhiye, R.S. Ningthoujam, Asar Asar Ahmed, D.K. Panda, S.S. Umre, S.J. Sharma, Pramana 70 (2008) 313–321.
[11] F. Dumestre, B. Chaudret, C. Amiens, P. Renaud, P. Fejes, Science 303 (2004) 821–823.
[12] F. Caruso, R.A. Caruso, H. Mohwald, Science 282 (1998) 1111–1114.
[13] L. Manna, E.C. Scher, A.P. Alivisatos, J. Am. Chem. Soc. 12 (2000) 12700–12706.
[14] R.S. Ningthoujam, N.S. Gajbhiye, Asar Asar Ahmed, S.S. Umre, S.J. Sharma, J. Nanosci. Nanotechnol. 8 (2008) 3059–3062.
[15] C.H.B. Ng, W.Y. Fan, J. Phys. Chem. B 110 (2006) 20801.
[16] F.C. Akkari, M. Kanzari, Phys. Status Solidi A 207 (2010) 1647.
[17] M. Hayashi, K. Katsuki, J. Phys. Soc. Japan 5 (1950) 380.
[18] K. Mizuno, M. Izaki, K. Murase, T. Shinagawa, M. Chigane, A. Tasaka, Y. Awakura, J. Electrochem. Soc. 152 (2005) C179.
[19] B.P. Rai, Sol. Cells 25 (1988) 265 1.
[20] R.N. Briskman, Sol. Energy Mater. Sol. Cells 27 (1992) 361.
[21] P.E. de Jongh, D. Vanmaekelbergh, J.J. Kelly, Chem. Commun. (1999) 1069.
[22] J. Zhang, J. Liu, Q. Peng, X. Wang, Y. Li, Chem. Mater. 18 (2006) 867.
[23] H. Xu, W. Wang, W. Zhu, J. Phys. Chem. B 110 (2006) 13829.
[24] B. White, M. Yin, A. Hall, D. Le, S. Stolbov, T. Rahman, N. Turro, S. O'Brien, Nano Lett. 6 (2006) 2095.
[25] P. Poizot, S. Laruelle, S. Grugeon, L. Dupont, J.M. Taracon, Nature 407 (2000) 496.
[26] Y. Chang, J.J. Teo, H.C. Zeng, Langmuir 21 (2005) 1074.
[27] J.J. Teo, Y. Chang, H.C. Zeng, Langmuir 22 (2006) 7369.
[28] L. Gou, C.J. Murphy, J. Mater. Chem. 14 (2004) 735.
[29] M.J. Siegfried, K.S. Choi, Angew. Chem. Int. Ed. 44 (2005) 3218.
[30] Y. Chang, H.C. Zeng, Cryst. Growth Des. 4 (2004) 273.
[31] H. Yanagimoto, K. Akamatsu, K. Gotoh, S. Deki, J. Mater. Chem. 11 (2001) 2387.
[32] R.V. Kumar, Y. Mastai, Y. Diamant, A. Gedanken, J. Mater. Chem. 11 (2001) 1209.
[33] S. Deki, K. Akamatsu, T. Yano, M. Mizuhata, A. Kajinami, J. Mater. Chem. 8 (1998) 1865.
[34] W. Wang, G. Wang, X. Wang, Y. Zhan, Y. Liu, C. Zhang, Adv. Mater. 14 (2002) 67.

[35] L.N. Huang, H.T. Wang, Z.B. Wang, A. Mitra, D.Y. Zhao, Y.S. Yan, Chem. Mater. 14 (2002) 876.
[36] M.J. Siegfried, K.S. Choi, Adv. Mater. 16 (2004) 1743.
[37] H. Li, R. Liu, R. Zhao, Y. Zheng, W. Chen, Z. Xu, Cryst. Growth Des. 6 (2006) 2795.
[38] J.A. Gadsden, Infrared Spectra of Minerals and Related Inorganic Compounds, Butterworths, USA, 1975, p. 44.
[39] M.B. Mahajan, M.S. Pavan, P.A. Joy, Solid State Commun. 149 (2009) 2199–2201.
[40] J. Ghijsen, L.H. Tjeng, J. van Elp, H. Esks, J. Westerink, G.A. Sawatzky, Phys. Rev. B 38 (1988) 11322.
[41] J. Wang, L. Li, D. Xiong, R. Wang, D. Zhao, C. Min, Y. Yu, L. Ma, Nanotechnology 18 (2007) 075705.